PROGRESS IN ATOMIC ABSORPTION SPECTROSCOPY EMPLOYING FLAME AND GRAPHITE CUVETTE TECHNIQUES

B. V. L'VOV

Commission on Spectroscopy, U.S.S.R. Academy of Sciences, Moscow

ABSTRACT

A simplified theory of analytical signal formation for various methods of sample atomization is proposed which takes into account the nature of sample transfer through the analytical cell and instrumental distortions of the pulse shape. An analysis of the relationships obtained shows the essential advantages of the integral absorption recording method over conventional equilibrium and peak methods. These advantages were employed to simplify the standardization procedure in the determination of impurities in the cuvette (10^{-5} to 10^{-8} per cent) and to develop a method of analysing solid samples by the flame technique using electric heating. The proposed theory also permitted optimization of the conditions of cuvette measurement by the peak method, making it possible to achieve record low absolute detection limits (10^{-14} to 10^{-15} g) and to reduce random measurement error to two per cent.

The 'transparency' of the graphite cuvette in the vacuum spectral region was used for direct determination by atomic absorption spectroscopy of sulphur, phosphorus and iodine by their resonance lines. A possibility was established of determining phosphorus and iodine by non-resonance lines P 2136 Å and I 2062 Å.

A method is described for determining relative oscillator strengths f in the spectra of elements from the absorption sensitivities of various lines measured by the flame technique. A comparison of the f values calculated from published sensitivity data with the most reliable values confirms the validity of the method.

Attention will be drawn to several problems in atomic absorption spectroscopy the actual selection of which in no way reflects the general progress achieved in this field in recent years. It will be rather a report on the research carried out in our laboratory during the last two years.

THEORY OF THE SHAPE OF ANALYTICAL SIGNALS

Despite a large number of attempts to employ various atomization methods to produce an absorbing layer of atomic vapours this problem still remains unresolved. In our opinion, the reason for this lies in the purely empirical approach to its solution which has proved to be sufficient when developing emission techniques of analysis. Paradoxical as this may seem, the selection of an optimum method of atomization in atomic absorption

11

spectroscopy represents a much more complicated problem. The fact is that atomic absorption analysis reveals trends to considerable instrumental and methodological simplifications manifesting themselves in rejection of the principles involving the use of internal standards and reference samples similar in composition to the sample to be analysed.

If one rejects these principles (completely or partially), more rigorous requirements should be imposed on the methods of atomization. Turning to evaluation or selection of an atomization method suitable for atomic absorption analysis we have to find out, in the first place, whether it is possible to choose such conditions of sample atomization that would guarantee a composition-independent, unambiguous correspondence between the magnitude of the analytical signal measured and the content of element in the sample.

It should be noted that a direct approach to this problem consisting of an attempt to find, for each atomization method considered, 'coupling equations' which would relate the analytical signal to the concentration of element in the sample is, in our opinion, inadequate, First of all, the process of transfer of a substance into the analytical cell is affected by a vast number of factors determined by both the performance of atomizers and sample characteristics, e.g. the physicochemical properties of the sample, the shape and condition of its surface (when solid samples are atomized), chemical composition etc. whose proper consideration would hardly be possible. Secondly, even if such a coupling equation were found, it would still not be clear how to use it for analysis since the physicochemical properties of a sample and even its approximate chemical composition are usually unknown.

A more natural and practical approach lies in establishing such atomization conditions and methods of analytical signal recording that would not depend on possible variations in sample composition and properties and on uncontrollable changes in the parameters of the atomization method. To do this, we shall use an extremely simplified model in order to express mathematically the process of change of the number of atoms in the analytical cell with a subsequent analysis of the relationships obtained.

For the sake of simplicity, we shall restrict ourselves to considering only the processes of the transfer of sample vapour through the analytical cell while eliminating all the intermediate stages in transformation of the sample before it enters the cell. Also we shall not deal with any process accompanying the transfer of substance through the cell, such as dissociation of molecules, excitation and ionization of atoms, but assume the element of interest in the cell to be in the atomic state. Such an approach is sound enough since the processes excluded from consideration are easily controlled. Thus, we limit ourselves to a study of only those factors which manifest themselves via a change in the *conditions of transfer* of a sample through the cell. Such changes can, in principle, be due both to variations in sample composition and uncontrollable differences in equipment used for atomization.

At any moment of time during the presence of the element in question in the analytical cell the operator can record the analytical signal which is, however, related directly only to the *element content in the cell* at the given

12

moment. The purpose of our analysis is to find which particular characteristic of an analytical signal should be recorded, at what moment and for how long, as well as the conditions which should be maintained in order that the measured data will be unambiguously related to the *element content in the sample*, but independent of, or depending as little as possible on, variations in the conditions of transfer. Another aspect of this study that is by no means less important is a determination of analytical conditions which will ensure maximum sensitivity and precision.

We shall consider the process of substance transfer through the cell, using the concepts developed by S. L. Mandelstam[1] and later by Ya. D. Reichbaum[2]. We shall understand the cell to be the analytical volume involved directly in the formation of the analytical signal observed experimentally. We introduce the following notation:

N_0 the number of atoms of the element under study in the consumed sample;

N total number of atoms of the element under study in the cell at the moment of time t;

τ_1 duration of transfer of atoms into the cell;

τ_2 average time of residence of atoms in the cell;

τ_3 signal recording duration.

The balance between the number of atoms entering the cell $n_1(t)$ and those escaping from it $n_2(t)$ can obviously be expressed by the following equation

$$dN/dt = n_1(t) - n_2(t) \tag{1}$$

The form of the functions $n_1(t)$ and $n_2(t)$ depends on the actual method of atomization used. Naturally, the flame and graphite cuvette techniques are of major interest here. With a mechanical method of sample transfer to the cell which is used in practice in all flame analyses

$$n_1(t) = N_0/\tau_1 \tag{2}$$

and

$$n_2(t) = (w/v)N = N/\tau_2 \tag{3}$$

where w/v is the ratio of the volume of aerosol-containing gas introduced per unit time to that of the analytical cell. In burners with premix chambers, which have found widespread use, the functions of the analytical cell are performed by the chamber proper. Since element concentrations in the chamber and in the region of the flame under study there are related by a coefficient of proportionality, we may, in our consideration of the changes in the signal, confine ourselves to a study of concentration changes in the premix chamber.

In the thermal method of sample introduction into the cell used with the graphite cuvette, evaporation occurs at a constantly increasing evaporator temperature, so that the process of sample introduction can be approximated as a linear function of time

$$n_1(t) = At \tag{4}$$

13

From the condition of normalization

$$\int_0^{\tau_1} n_1(t)\,dt = N_0 \tag{5}$$

we find

$$n_1(t) = (2N_0/\tau_1^2)\,t \tag{6}$$

Sample atoms escape from the cuvette by vapour diffusion through openings, so that

$$n_2(t) = N/\tau_2 \tag{7}$$

Thus equation 1 for flame atomization can be written in the form

$$(dN/dt) = (N_0/\tau_1) - (N/\tau_2) \tag{8}$$

and for the cuvette,

$$(dN/dt) = (2N_0/\tau_1^2)t - (N/\tau_2) \tag{9}$$

Solving these equations yields formulae which describe the kinetics of the change in the number of atoms in the analytical cell for the specified methods of sample atomization (column 3 of *Table 1*).

The following point deserves attention at this stage. Electronic circuits used to record analytical signals introduce distortions into the original pulse shape. Consideration of the distortion of a pulse passing through *RC* circuits with a capacitor at the output, which are always present in any photoelectric recording device and serve to cut off the noise accompanying the signal to be measured is of major interest. From the theory of electric networks (see, for instance, ref. 3) it is known that the shape of distorted signal $i(t)$ is related to the original signal shape $N(t)$ and the transient characteristic of the network $A(t)$ describing distortion of a unit voltage jump by the following formula

$$i(t) = N(0) \times A(t) + \int_0^t A(t - \tau)N'(\tau)\,d\tau \tag{10}$$

where τ is an integration variable, $N'(\tau)$ is a derivative of the function $N(t)$ with the argument t replaced by the variable τ, and $N(0)$ is the value of the function $N(t)$ at the moment $t = 0$.

The transient characteristic of an *RC* circuit having a capacitor at the output with the voltage jumping from zero to unity is expressed by the formula

$$A(t) = 1 - \exp\left(-t/\tau_{\text{cir}}\right) \tag{11}$$

and with the voltage jumping from unity to zero, by

$$A(t) = \exp\left(-t/\tau_{\text{cir}}\right)$$

Here τ_{cir} is the time constant of the circuit

$$\tau_{\text{cir}} = RC \tag{12}$$

Using equation 10, calculations for each part of the pulse $N(t)$ give final

14

Table 1. Pulse shapes under various conditions of sample introduction into the cell

Mode of introduction	Time interval	Initial, $N(t)$	Pulse — Distorted, $i(t)$
Uniform, $n_1(t) = \dfrac{N_0}{\tau_1}$	$t \leqslant \tau_1$	$N_0 \dfrac{\tau_2}{\tau_1}\left(1 - e^{-\frac{t}{\tau_2}}\right)$	$N_0 \dfrac{\tau_2}{\tau_1}\dfrac{\tau_2\left(1 - e^{-\frac{t}{\tau_2}}\right) - \tau_{cir}\left(1 - e^{-\frac{t}{\tau_{cir}}}\right)}{\tau_2 - \tau_{cir}}$
	$t \geqslant \tau_1$	$N_0 \dfrac{\tau_2}{\tau_1}\left(1 - e^{-\frac{\tau_1}{\tau_2}}\right)e^{-\frac{t-\tau_1}{\tau_2}}$	$N_0 \dfrac{\tau_2}{\tau_1}\dfrac{\tau_2\left(1 - e^{-\frac{\tau_1}{\tau_2}}\right)e^{-\frac{t-\tau_1}{\tau_2}} - \tau_{cir}\left(1 - e^{-\frac{\tau_1}{\tau_{cir}}}\right)e^{-\frac{t-\tau_1}{\tau_{cir}}}}{\tau_2 - \tau_{cir}}$
Accelerated, $n_1(t) = \dfrac{2N_0}{\tau_1^2}t$	$t \leqslant \tau_1$	$N_0 \dfrac{2\tau_2^2}{\tau_1^2}\left(\dfrac{t}{\tau_2} - 1 + e^{-\frac{t}{\tau_2}}\right)$	$N_0 \dfrac{2\tau_2}{\tau_1^2}\dfrac{\tau_2^2\left(\dfrac{t}{\tau_2} - 1 + e^{-\frac{t}{\tau_2}}\right) - \tau_{cir}^2\left(\dfrac{t}{\tau_{cir}} - 1 + e^{-\frac{t}{\tau_{cir}}}\right)}{\tau_2 - \tau_{cir}}$
	$t \geqslant \tau_1$	$N_0 \dfrac{2\tau_2^2}{\tau_1^2}\left(\dfrac{\tau_1}{\tau_2} - 1 + e^{-\frac{t}{\tau_2}}\right)e^{-\frac{t-\tau_1}{\tau_2}}$	$N_0 \dfrac{2\tau_2}{\tau_1^2}\dfrac{\tau_2^2\left(\dfrac{\tau_1}{\tau_2} - 1 + e^{-\frac{\tau_1}{\tau_2}}\right)e^{-\frac{t-\tau_1}{\tau_2}} - \tau_{cir}^2\left(\dfrac{\tau_1}{\tau_{cir}} - 1 + e^{-\frac{\tau_1}{\tau_{cir}}}\right)e^{-\frac{t-\tau_1}{\tau_{cir}}}}{\tau_2 - \tau_{cir}}$

expressions for the distorted shape of the pulse $i(t)$ as shown in the last column of *Table 1*.

METHODS OF ATOMIC ABSORPTION RECORDING

We turn now to an analysis of the above relationships. First of all we shall consider the methods of recording analytical signals which permit information on the content of element in the sample to be obtained. As an example, *Figure 1* presents the shapes of the pulses $N(t)$ observed with N_0
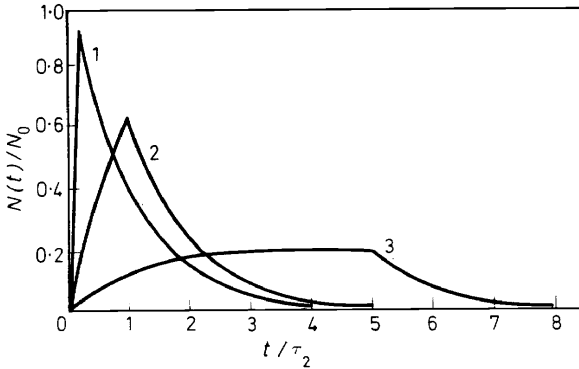
Figure 1. Pulse shapes for various τ_1/τ_2 ratios: $1-\tau_1/\tau_2 = 0.2$; $2-\tau_1/\tau_2 = 1$; $3-\tau_1/\tau_2 = 5$

atoms of the element under study introduced uniformly in three cases with differing magnitudes of the ratio τ_1/τ_2. As can be seen from the figure, at least two quantities can be used to characterize the pulses, namely, the peak value $N_{max.}$ corresponding to the peak of the pulse, and the integral quantity Q_N representing the pulse area

$$Q_N \equiv \int_0^{\tau_3} N(t)\, \mathrm{d}t \qquad (13)$$

Besides, from a consideration of the longer pulse in *Figure 1* it can be seen that at large τ_1/τ_2, as t increases, the magnitude of $N(t)$ approaches some *equilibrium value* N_{eq} corresponding to the condition

$$\mathrm{d}N/\mathrm{d}t = 0 \qquad (14)$$

From equation 8 with condition 14 it follows that

$$N_{eq} = (\tau_2/\tau_1)\, N_0 \qquad (15)$$

Of the above methods of signal recording in atomic absorption analysis the most widely used are the equilibrium method in the flame technique[11] and the peak method employed with the cuvette technique[12]. Quite recently, the peak method of recording in combination with sample evaporation from a tantalum boat was used in flame analysis[4], and the equilibrium method with mechanically introduced aerosol in the graphite cuvette technique[5].

The use of an integral method of pulse recording in atomic absorption spectroscopy with samples evaporated from a graphite cuvette was reported

16

for the first time by Massmann[6]. An attempt to employ an integrating circuit in atomic absorption measurements with an arc atomizer has also been reported[7]. However, the authors integrated the signal in the difference of intensities rather than in optical density which, as we shall see later, is less effective.

The advantages of the integral method over the peak method of recording were first pointed out clearly by the present author[9]; a detailed mathematical analysis of the method together with an experimental confirmation of its advantages in the case of the graphite cuvette has also been given[8]. An independent experimental verification of some advantages offered by the integral method when working with the cuvette was reported at the same time[10]. Finally, application of the integral method of recording in flame analysis has also been given for the first time[13].

THE INTEGRAL METHOD OF RECORDING ABSORPTION

Now what are the above-mentioned advantages of the integral method of recording? To answer this question, let us turn to the formulae given in *Table 1*. An integration of the functions describing the pulse shape for the above models of sample transfer readily shows that in both cases

$$Q_N = \int_0^\infty N(t)\, dt = \int_0^\infty i(t)\, dt = N_0\tau_2 \tag{16}$$

which apparently permits generalizing this result to any process of substance transfer irrespective of the actual form of the function $n_1(t)$ in equation 1.

The vital feature of formula 16 is that the integral value of the signal is independent of the rate and duration of sample introduction into the analytical cell, as well as of parameters of the recording circuit (τ_{cir}). This is very important since, first, the measurement of Q permits one to prevent varying sample composition from affecting the analytical results and, secondly, by increasing the duration of a measurement one can increase the amount of the substance used for an analysis, and hence increase the relative sensitivity of the analysis. The only condition to be fulfilled here is to maintain the *magnitude of τ_2 constant* and, of course, to ensure *complete evaporation of the element to be analysed*.

A few remarks concerning practical application of the method now follow. First, it follows from equation 16 that the signal should be integrated in units proportional to $N(t)$, i.e. in optical density. Replacing the quantities $N(t)$ and N_0 by the corresponding optical densities $D(t)$ and D_0, formula 16 can be rewritten as follows

$$Q_D \equiv \int_0^\infty D(t)\, dt = D_0\tau_2 \tag{17}$$

Secondly, it is required that the magnitude of Q_D measured in practice (during a finite time interval τ_3) should be sufficiently close to its limiting value at infinite investigation time. From an analysis of the formula below corresponding to the simplest case of uniform sample introduction at $\tau_{cir} = 0$

$$\int_0^{\tau_3} D(t)\, dt = D_0\tau_2[1 - (\tau_2/\tau_1)(1 - e^{-\tau_1/\tau_2})\, e^{-(\tau_3-\tau_1)/\tau_2}] \tag{18}$$

17

it follows that the difference between the magnitudes $\int_0^{\tau_3} D(t)\, dt$ and $D_0\tau_2$ does not exceed two per cent provided the condition

$$\tau_3 \geqslant \tau_1 + 4\tau_2 \qquad (19)$$

is fulfilled.

In order to check the principal formula 17, the following experiment was carried out[8]. Equal amounts of an element in a cuvette were evaporated

Table 2. Integrated absorption for various rates of sample evaporation*

$D_{max.}$	Q_D (opt. dens. × sec)	$D_{max.}$	Q_D (opt. dens. × sec)
0·72	1·7	0·24	1·7
0·66	1·7	0·16	1·7
0·51	1·8	0·13	1·9
0·32	2·0	0·09	1·7

* Experimental: cuvette 2·5 mm diameter, 40 mm length; $T = 1\,400°C$, $P = 4$ atm. The absorption was measured at $\lambda\, 2\,768$ Å for $2·5 \times 10^{-10}$ g Tl.

at different levels of additional electrode heating and without additional heating at all. The peak value of absorption $D_{max.}$ and the integral value Q_D (see Table 2) were measured for each pulse. It can be seen that despite a considerable difference in sample evaporation rates, reflected indirectly in the magnitude of $D_{max.}$, the value of Q_D remains practically constant. Thus, the integral method of recording indeed permits one to exclude the effect of kinetics of sample transfer to the analytical cell on the measured results.

To evaluate the practical advantages of the integral recording method, we shall consider two analytical problems, namely, the determination of impurities in highly pure materials by means of the graphite cuvette technique, and the direct analysis of solid samples by the flame technique.

In impurity determination in low-volatile powder samples, evaporation of the elements in question from the matrix can proceed much more slowly than with these elements deposited on the electrode in solution form. This should result in a decrease of the peak absorption value $D_{max.}$ and hence in the appearance of systematic errors. Therefore, calibration by means of pure solutions of elements cannot be used in this case. Application of the integral method of recording permits one to disregard differences in element evaporation rate in the pure form and from a powder sample thus simplifying the problem of standardization.

This advantage of the method was exploited by D. A. Katskov and the author in a determination of impurities in graphite powder. To prevent vapour from escaping through porous electrode walls electrodes of impermeable pyrographite were used. About 8 mg of powdered sample was introduced into a bore in the electrode which was 3 mm deep and 2 mm in diameter.

Experimental conditions and the results of the impurity determination in graphite are presented in Table 3. The last column of the table contains

18

Table 3. Determination of impurities in graphite

Line, Å	T, °C	Concentration, %		$Q_{min.}$	Limit of detection, %
		Common graphite	Purified graphite		
Co 2407	2200	$5 \cdot 3 \times 10^{-7}$	$<1 \times 10^{-7}$	0·013	1×10^{-7}
Mn 2795	2000	$5 \cdot 6 \times 10^{-7}$	9×10^{-8}	0·005	1×10^{-8}
Ni 2320	2000	$<9 \times 10^{-7}$	$<5 \times 10^{-7}$	0·0024	5×10^{-7}
Fe 2483	2100	$>1 \times 10^{-3}$	$4 \cdot 3 \times 10^{-6}$	0·024	5×10^{-7}
Cu 3248	2100	$1 \cdot 5 \times 10^{-6}$	$<5 \times 10^{-7}$	0·014	5×10^{-7}
Zn 2139	1500	$1 \cdot 3 \times 10^{-5}$	$3 \cdot 4 \times 10^{-7}$	0·0046	2×10^{-8}

relative limits of detection of these elements corresponding to the criterion[14] $Q_{b1} + 2\sigma_{b1}$.

We shall now consider the possibility of applying the integral recording method to the flame technique. The principal limitations of the conventional flame technique consist of a low efficiency with which the sample is used manifesting itself in low absolute and relative sensitivity, and of the effect of incomplete evaporation of the aerosol on analytical results and inapplicability of this technique to direct analysis of solid samples. In connection with these limitations, a proposal was made[13] to use in flame absorption measurements the integral method in combination with direct evaporation of the sample into the flame. The case of magnesium determined in a 100-fold amount of aluminium nitrate confirmed the independence of the measurement data on variations in evaporation rate of the element to be analysed caused by the presence of other components in the sample. However, the method of sample evaporation from a tungsten wire heated with an air-acetylene flame used by L'vov and Plushch[13] turned out to inapplicable to evaporation of low- and medium-volatile elements, as well as for direct introduction of solid samples into the flame. Therefore, in later work[15] samples were evaporated into the flame by means of a graphite furnace heated independently with alternating current.
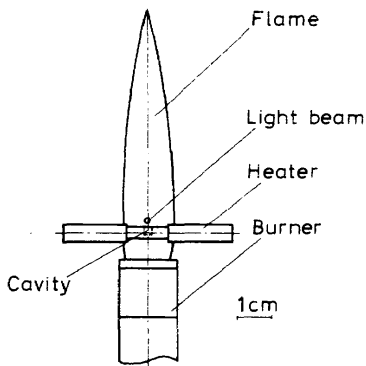
Figure 2. Atomizer arrangement

The arrangement of a graphite heater, the flame and the light beam is shown in *Figure 2*. The shape of the graphite rod was chosen so as to ensure maximum possible heating of the bore with the sample. The light beam was focused into a spot 2 to 3 mm in diameter and 1 to 2 mm above the bore. The rod ends were fixed in water-cooled metal contacts. The current flowing through the rod (up to 200 A) was controlled by varying the voltage across the primary of a step-down transformer.

The analytical procedure was as follows. The rods were first heated under the same conditions at which the analysis was later carried out. When solutions were analysed, the electrode bore was treated with a drop of polystyrene dissolved in benzene, after which a few microlitres of solution were placed into the bore by means of a micropipette. The drop was then evaporated and the rod was fixed in the stand. With solid samples, a weighed amount of powdered sample and graphite was placed into the bore. The actual dilution of the material to be analysed with graphite and the weight of the sample were chosen so that the expected content of the element in question in the sample should lie within the range convenient for the measurement of Q_D. For instance, in a determination of 0·003 per cent copper a tenfold dilution (in weight), was used, the sample being 5 mg in weight.
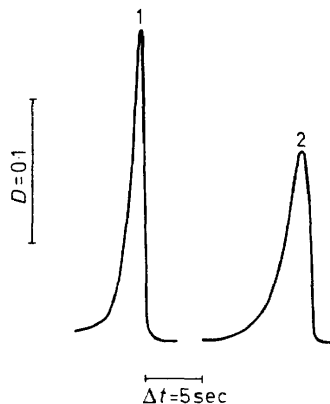
Figure 3. Absorption pulse records in copper determination: 1—solution form; 2—ZnO powder mixed with graphite

On fixing the rod in the stand, the position of the bore was checked with respect to the light beam passing above the rod. The burner with the flame was placed under the rod, its heating being turned on at the same time. The duration of heating was checked by the pattern of signal variation on the recorder chart (*Figure 3*). As soon as the pen returned to the original level, the heating was turned off, and the flame was moved aside.

Summarized in *Table 4* are the results of copper determinations in various powdered materials. The content was calculated using a calibration graph drawn for a pure copper solution. Fairly good agreement between the measurement data and real contents of the element in the samples is a further confirmation of the principal advantage of the integral absorption

Table 4. Determination of copper in solid materials

Sample	Copper concentration, %		Sample	Copper concentration, %	
	given	*found*		*given*	*founa*
MgO	0·003	0·0027	Al–Mg ferrite	0·003	0·0034
Fe_2O_3	0·003	0·0028	Ni–Zn ferrite	0·003	0·0030
Cr_2O_3	0·003	0·0027	$BaCO_3$	0·003	0·0029
Al_2O_3	0·003	0·0028	$BaCO_3$	0·01	0·0088
ZnO	0·003	0·0027			

recording method because the analytical results were independent of sample composition.

The standard deviation for a single determination is five per cent for solutions and ten per cent for solid samples. We believe that an application of an electronic integrator (in our work[13, 15] 'weighing' of the pulse area was used) and a dual-beam spectrophotometer should markedly improve the precision.

The absolute sensitivity of the method reduced to terms of one per cent absorption in one second, i.e. to $Q_D = 0·0043$ sec, is quite high: Mg 2852 Å— 4×10^{-11} g, Mn 2795 Å—2×10^{-10} g, Co 2407 Å—3×10^{-10} g, Cu 3248Å —4×10^{-10} g, Ag 3281 Å—5×10^{-11} g, Pb 2833 Å—4×10^{-10} g. Considering the possibility of evaporating samples of a few milligrammes and the above absolute sensitivity, one can expect to achieve a relative sensitivity of about 10^{-6} to 10^{-4} per cent for a solid sample.

The range of elements determined by the above method is restricted at present to the conventional list of high-volatile and medium-volatile elements measured in the air–acetylene flame. The use of high-temperature flames could probably extend it to low-volatile elements such as aluminium, vanadium, etc.

The above results can apparently be summed up in the following way. The solution to the problem of sample atomization in atomic absorption analysis should be sought not in a development of essentially novel atomization techniques, but rather in a reasonable *combination of already known devices* (flame and graphite cuvette) supplemented by various methods of analytical signal recording and, first, by *the integral method.*

OPTIMIZATION OF MEASUREMENT CONDITIONS

Now I should like to discuss some other aspects of the use of the above theory of analytical signal shaping associated with the optimization of analytical conditions. Because of shortage of time, we shall deal with two problems only, namely, achieving the lowest absolute limits of detection and increasing precision with the graphite cuvette technique. In doing this we shall isolate out of all the factors affecting these characteristics only one, namely, *selection of optimum parameters of the recording circuit from the viewpoint of reaching the highest possible signal-to-noise ratio* with the peak recording technique.

The value of the signal at the maximum of the pulse, taking into consideration pulse shape distortion due to a finite τ_{cir} can be found from the formulae

in *Table 1*. To do this, we shall use the following formula expressing the variation of signal amplitude at uniformly-accelerated sample evaporation at the moment of time $t \geqslant \tau_1$

$$D(t)_{t > \tau_1} = D_0 \frac{2\tau_2}{\tau_1^2}$$

$$\times \frac{\tau_2^2 \left\{ \frac{\tau_1}{\tau_2} - 1 + e^{-\tau_1/\tau_2} \right\}^{-(t-\tau_1)/\tau_2} - \tau_{cir}^2 \left\{ \frac{\tau_1}{\tau_{cir}} - 1 + e^{-\tau_1/\tau_{cir}} \right\} e^{-(t-\tau_1)/\tau_{cir}}}{\tau_2 - \tau_{cir}} \quad (20)$$

From the condition

$$(d/dt)\, D(t) = 0 \quad (21)$$

we find the value of $t_{max.}$ corresponding to the pulse maximum

$$t_{max.} = \frac{\tau_2 \tau_{cir}}{\tau_2 - \tau_{cir}} \ln \frac{\tau_1 e^{\tau_1/\tau_{cir}} - \tau_{cir} e^{\tau_1/\tau_{cir}} + \tau_{cir}}{\tau_1 e^{\tau_1/\tau_2} - \tau_2 e^{\tau_1/\tau_2} + \tau_2} \quad (22)$$

Substituting equation 22 into 20 we get the desired expression

$$D_{max.} = D_0 \eta \left(\frac{\tau_1}{\tau_2}, \frac{\tau_{cir}}{\tau_2} \right) \quad (23)$$

where

$$\eta \left(\frac{\tau_1}{\tau_2}, \frac{\tau_{cir}}{\tau_2} \right) \equiv \frac{2\tau_2^2}{\tau_1^2} \left(\frac{\tau_1}{\tau_2} e^{\tau_1/\tau_2} - e^{\tau_1/\tau_2} + 1 \right)^{\tau_2/(\tau_2 - \tau_{cir})}$$

$$\times \left(\frac{\tau_1}{\tau_2} e^{\tau_1/\tau_{cir}} - \frac{\tau_{cir}}{\tau_2} e^{\tau_1/\tau_{cir}} + \frac{\tau_{cir}}{\tau_2} \right)^{-\tau_{cir}/(\tau_2 - \tau_{cir})} \quad (24)$$

From formula 24 it follows that the magnitude of η, and hence the magnitude of $D_{max.}$, decreases with increasing τ_{cir} (the value of τ_2 being assumed constant), i.e. that the sensitivity of measurements decreases. Because of this, in our earlier work we always chose $\tau_{cir} \ll \tau_2$. However, from the viewpoint of the highest signal-to-noise ratio (S/N) such a choice of τ_{cir} is wrong. Indeed, it is well known (see, for instance, ref. 17) that the noise is also a decreasing function of τ_{cir}, and, furthermore,

$$N \propto 1/\sqrt{\tau_{cir}} \quad (25)$$

Therefore, from the S/N ratio viewpoint the optimum value of τ_{cir} should be found from the condition of maximum of the function

$$\frac{S}{N} \propto \frac{\eta \left(\frac{\tau_1}{\tau_2}, \frac{\tau_{cir}}{\tau_2} \right)}{\sqrt{(\tau_{cir}/\tau_2)}} = \eta \left(\frac{\tau_1}{\tau_2}, \frac{\tau_{cir}}{\tau_2} \right) \bigg/ \sqrt{\frac{\tau_{cir}}{\tau_2}} \quad (26)$$

The dependence of this function on τ_{cir}/τ_2 for various values of τ_1/τ_2 computed by D. A. Katskov and the present author is shown in *Figure 4*.
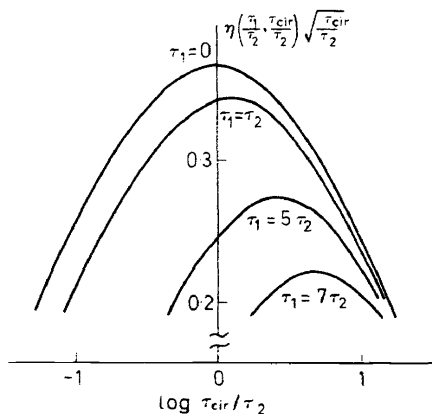
Figure 4. Relationship $\eta\left(\dfrac{\tau_1}{\tau_2}, \dfrac{\tau_{cir}}{\tau_2}\right) \Big/ \sqrt{\dfrac{\tau_2}{\tau_{cir}}}$ versus $\dfrac{\tau_{cir}}{\tau_2}$ for various values of τ_1/τ_2

As can be seen from the figure, the maximum value of S/N at $\tau_1/\tau_2 = 0$ corresponds to

$$\tau_{cir} = \tau_2 \qquad (27)$$

As τ_1/τ_2 increases, the maximum of the function shifts somewhat to larger τ_{cir}. In practice, however, in the case of evaporation into the cuvette of samples deposited in solution form on the electrode face, one almost always has $\tau_1/\tau_2 < 1$. Therefore, for the optimization of measurement conditions it is sufficient to satisfy condition 27.

$\tau_{cir} = 0 \cdot 08$ sec

$\tau_{cir} = 0 \cdot 7$ sec
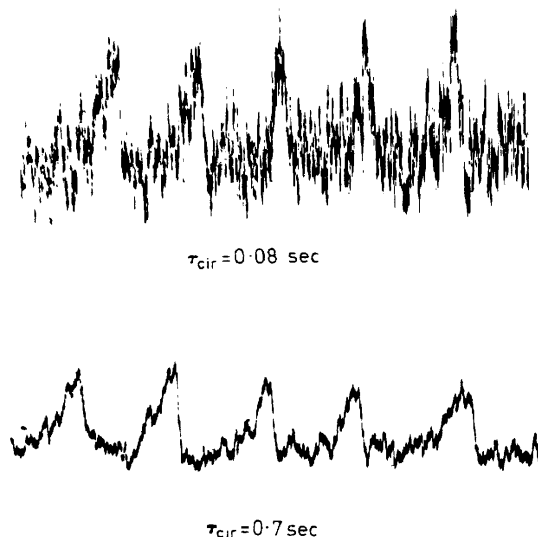
Figure 5. Pulse records for various values of τ_{cir}

23

As an example illustrating the effect of τ_{cir} on the signal-to-noise ratio in atomic absorption measurements of the peak values of pulses, *Figure 5* shows recordings of a series of pulses obtained at different values of τ_{cir} (the other parameters remaining unchanged). A comparison of the records shows a clear improvement in the signal-to-noise ratio despite some decrease in pulse amplitude with increasing τ_{cir}. Thus *to achieve the lowest detection limit with the graphite cuvette when using the peak recording technique, one should choose the time constant of the recording circuit close to the magnitude of* τ_2. Of course, this is not the only requirement imposed on the measurement conditions for the lowest possible amounts of elements; however, a more detailed consideration of these requirements would lead us too far away from our principal subject. It should be noted, however, that in the experiments carried out by D. A. Katskov and the author[18] and described below which were aimed at achieving the lowest detection limits, the majority of the parameters were likewise chosen to be optima.

Ultrasmall amounts of cadmium, manganese and silver were determined. Solutions of the corresponding elements were deposited on the electrode faces by means of a micropipette capable of dosing drops as small as 0·017 μl in volume with an error of 20 per cent. Conventional equipment was used in the measurements[9, 15]. For light sources we used h.f. lamps (Cd, Mn) and a hollow-cathode lamp (Ag) powered with pulsed current[19]. A cuvette 0·4 mm in diameter and 20 mm long was made of impermeable graphite. The monochromator slit width (0·2 mm) corresponded approximately to the size of the light spot focused on the entrance slit. The amplifier time constant (0·5 sec) was close to the magnitude of τ_2.

Table 5 lists the other experimental conditions and the results obtained, and in *Figure 6* records are shown for the lowest amounts of the elements determined. The penultimate column contains the values of optical density corresponding to average values of the noise amplitude (ΔD), and the last column contains the detection limits corresponding to $2\Delta D$.

Table 5. Determination of ultra-low quantities of elements

Line, Å	T, °C	P, atm	M_{meas} g	D_{meas}	ΔD	$M_{2\Delta D}$, g
Cd 2 288	1400	1·2	$5·5 \times 10^{-15}$	0·0043	0·001	$2·8 \times 10^{-15}$
Mn 2 795	1900	2	8×10^{-14}	0·020	0·003	$2·4 \times 10^{-14}$
Ag 3 281	1900	2	5×10^{-14}	0·022	0·006	$2·7 \times 10^{-14}$

A comparison of the observed noise level with the value calculated from the known magnitudes of photocurrent and τ_{cir} has shown the observed signal fluctuations to be determined solely by the shot effect in the photomultiplier.

A comparison of this method with other sensitive analytical procedures (*Table 6*) confirms the advantages of the cuvette technique over all other modern methods in the field of microanalysis. This, in particular, enabled us to use this method successfully for the determination of the content of stable carrier elements in cyclotron-activated specimens of ^{109}Cd, ^{65}Zn, ^{125}Sb, etc.[20, 21].

24
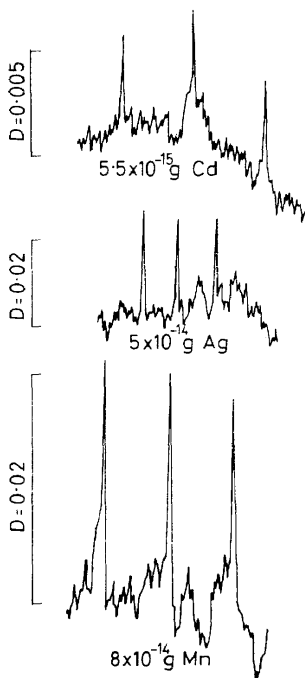
Figure 6. Records for trace determination

Table 6. Limits of detection (g) for Cd, Mn and Ag by various methods

| Element | Atomic absorption | | Emission | | |
	Cuvette	Flame	Arc	Flame	'Copper' spark
Cd	3×10^{-15}	3×10^{-10}	1×10^{-9}	1×10^{-7}	1×10^{-7}
Mn	2×10^{-14}	5×10^{-10}	1×10^{-8}	3×10^{-10}	3×10^{-9}
Ag	3×10^{-14}	1×10^{-9}	8×10^{-9}	1×10^{-9}	2×10^{-7}

| Element | Neutron activation | | Mass-spectrometry |
	2×10^{14} n/cm^2 . sec	5×10^{11} n/cm^2 . sec	
Cd	1×10^{-9}	5×10^{-7}	3×10^{-10}
Mn	1×10^{-12}	5×10^{-10}	5×10^{-11}
Ag	1×10^{-12}	1×10^{-9}	2×10^{-10}

Another result of recording circuit optimization (selection of $\tau_{\text{cir}} = \tau_2$) of importance in practice is a considerable improvement of precision with the graphite cuvette. Whereas in earlier days[16] a variation coefficient of 5 to 8 per cent was considered normal, now an increase of τ_{cir} up to 0·5 to 1 sec permitted reduction of the data spread from the mean to two per cent. A study of errors was carried out by D. A. Katskov and the author in the case of the silver determination. Experimental conditions were as follows: spectral line Ag 3281 Å, $T = 2100°\text{K}$, $P = 3$ atm, cuvette diameter 4·5 mm and length 40 mm, $\tau_{\text{cir}} = 1$ sec. The value of $D_{\text{max.}}$ at the introduction of 1×10^{-11} g Ag was approximately 0·3. The variation coefficient w_1 characterizing the reproducibility of data within the series of analyses and the variation coefficient w_2 characterizing deviation of results from the mean for all analyses were calculated from 100 parallel determinations of the same amount of silver (20 series of 5 analyses each) carried out during two days. The values obtained are $w_1 = 1\cdot8$ per cent, $w_2 = 3\cdot0$ per cent. The difference between them is due to factors changing slowly in time. In our opinion, the principal contribution to these variations is due to the instability of the amplifier logarithmic characteristic. By introducing temperature stabilization of the logarithmic circuit or taking into consideration variations of this characteristic by means of reference signals one should also eventually approach the error w_1 in measurements stretched out in time.

Of course, an improvement in the signal-to-noise ratio was not the only factor responsible for improved precision. As mentioned earlier[16], a marked contribution to the analytical errors has been introduced up to now by imperfect recording systems where a comparatively slow potentiometer (about one second for full-scale deflection) was used to record pulses with a very short rise time (of a few tenths of a second). An increase of τ_{cir} to one second resulted in such a distortion of the original pulse that the same recorder could hardly follow variations of the signal magnitude; this was a source of additional errors in the pulse peak recording.

In connection with this progress *one should reconsider the wide-spread opinion*[10, 16, 22] *that the cuvette technique is much inferior to the flame method with respect to precision.* Of course, this conclusion concerns only the analysis of solutions where accurate dosing is possible, and only that version of the cuvette technique[9, 16] where, in contrast to the versions of refs. 6 and 24, a reliable control of the parameters τ_1 and τ_2 can be assured.

In conclusion to this section, I should like to stress once more the vast potential of the above concept. In particular, application of the integral method of recording in the measurements of absolute oscillator strengths[23, 17, 16] offers a possibility of considerable improvements in the accuracy of this method.

MEASUREMENTS IN THE VACUUM SPECTRAL REGION

In the vacuum region of the spectrum lie resonance lines of gases, halogens, carbon, phosphorus, sulphur and the most sensitive resonance lines of mercury and arsenic. Experiments in this spectral region meet with considerable difficulties because of strong absorption of the light beam by oxygen contained in the air, the opaqueness of quartz and the unsuitability of conventional radiation receivers. However, the most essential limitation

with the flame atomization of samples is associated with a considerable increase of light absorption by 'hot' oxygen of the flame (from excited states of O_2). Therefore, with the exclusion of several works on arsenic determination and a single attempt at phosphorus determination using the line P 1775 Å with a through hollow cathode serving as atomizer[25] no systematic atomic absorption studies have been carried out in this spectral region.

We turn now to a description of the graphite cuvette technique as a means of atomization as applied to atomic absorption measurements in the vacuum region. These results have been obtained by A. D. Khartsyzov and the author[41].
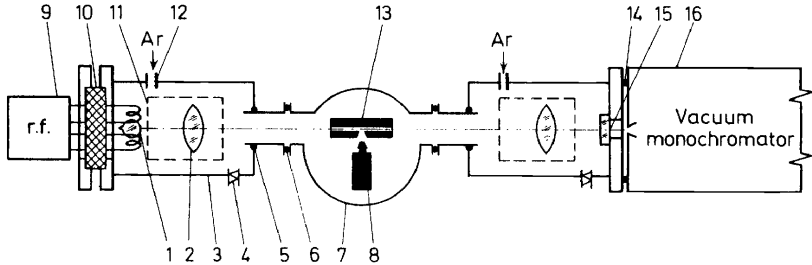
Figure 7. Spectrophotometer arrangement for atomic absorption measurements in the vacuum spectral region

Experiments were performed on laboratory equipment depicted schematically in *Figure 7*. Light source 1 and double-lens illumination system 2 of lithium fluoride are housed in two thin-walled cylindrical chambers 3 connecting with atomizer 7 through airtight seals 5, 6. The chambers were evacuated with a force pump and filled with argon via pipe sleeves 12. Controllable valves 4 serve for automatic release of excess argon pressure. Leads to the h.f. generator circuit 9 are passed through seal 10. Replacement of the light sources, control of their operation and lens adjustment in the chambers are carried out through windows 11 which are closed hermetically with lids of Plexiglas when in the operating condition. The right-hand chamber is connected to a vacuum monochromator 16 by means of a vacuum seal 14. The window 15 of lithium fluoride separates the chamber from the monochromator entrance slit. The cuvette 13 and electrodes 8 are housed in a chamber of conventional design[16, 26]. The illuminating system as a unit, 90 cm long, is fixed on the monochromator optical bench.

High frequency lamps made in our laboratory served as light sources. The measurement procedure was routine[16]. On fixing the electrodes with the samples in position, the equipment was evacuated and filled with argon to 1·2 atm. Measurements were carried out in a weak flow of argon. After each setting of the electrodes in the chamber the equipment could be made airtight in not more than one minute, and its evacuation and filling with argon took about two minutes. The cuvette temperature was maintained at 700°C for mercury determination and at 1 600°C when iodine, phosphorus and sulphur were being determined.

Table 7. Sensitivities for some resonance lines in vacuum

λ, Å	Transition	Low level energy, cm^{-1}	Sensitivity*
Hg 1849	$6s^2\ {}^1S_0\ -6p\ {}^1P_1$	0	$7{\cdot}0 \times 10^9$
I 1830	$5p^5\ {}^2P^0_{3/2}-6s\ {}^2P_{5/2}$	0	$1{\cdot}2 \times 10^8$
P 1775	$3p\ {}^4S^0_{3/2}-4s\,{}^4P_{5/2}$	0	$1{\cdot}3 \times 10^9$
P 1783	$3p\ {}^4S^0_{3/2}-4s\ {}^4P_{3/2}$	0	$1{\cdot}0 \times 10^9$
P 1788	$3p\ {}^4S^0_{3/2}-4s\ {}^4P_{1/2}$	0	$6{\cdot}0 \times 10^8$
S 1807	$3p\ {}^3P_2\ -4s\ {}^3S$	0	$5{\cdot}4 \times 10^7$
S 1821	$3p\ {}^3P_1\ -4s\ {}^3S$	398	$4{\cdot}2 \times 10^7$
S 1826	$3p\ {}^3P_0\ -4s\ {}^3S$	573	$1{\cdot}4 \times 10^7$
S 1900	$3p\ {}^3P_2\ -4s\ {}^5S$	0	$<10^5$

* Sensitivities are given in units of D/M ratio (optical density/g), for a cuvette 2·5 mm in diameter.

The results of sensitivity measurements for some lines are presented in *Table 7.* Calibration graphs for all elements are practically linear up to optical densities of 0·3 to 0·5. Experiments indicate the *possiblity of reliable determination of sulphur, phosphorus and iodine by the resonance lines* S 1807 Å, P 1775 Å and I 1830 Å with an absolute sensitivity of 8×10^{-11} g for S, 3×10^{-12} g for P and 4×10^{-11} g for I (with a cuvette 2·5 mm in diameter). The absolute sensitivity for the line Hg 1849 Å is 30 times that for Hg 2537 Å.

PHOSPHORUS AND IODINE DETERMINATION BY NON-RESONANCE LINES

Besides using the resonance lines of phosphorus and iodine in the vacuum region, there exists another possibility of determination of these elements by atomic absorption. From a consideration of the level diagram[32] for the neutral atoms P and I it is seen that relatively close ($\sim 1{\cdot}4$ eV) to the ground state $^2S_{3/2}$ of P there are located states $^2D^0_{3/2}$ and $^2D^0_{5/2}$, and at 0·94 eV from the ground state $^2P^0_{3/2}$ for I there lies the $^2P^0_{1/2}$ state. The population of the $^2D^0_{5/2}$ state at 2700°K should be about 0·4 per cent of the total number of phosphorus atoms, and that of the $^2P^0_{1/2}$ state, about one per cent of the total number of iodine atoms. Therefore, a possibility exists of observing atomic absorption for transitions to this state with the corresponding lines lying in the u.v. region of the spectrum. This possibility was studied by A. D. Khartsyzov and the author[27, 28]. Conventional equipment was used in the measurements[16, 17]. The spectrum of iodine has only one line at 2061·63 Å associated with the $^2P^0_{1/2}$ state. In the spectrum of phosphorus, a group of lines specified in *Table 8* was studied. The most sensitive was the line at 2136·18 Å (in practice absorption measurements were carried out for the doublet 2136·18 Å and 2135·47 Å which could not be resolved by the monochromator).

The populations of the lower levels of the lines studied, and hence the sensitivity of atomic absorption measurements by these lines, depend on the temperature by Boltzmann's law. This is clearly seen in *Figure 8* by comparing experimental data (points) with theoretical predictions (solid line). Some deviation of the experimental data from the upper part of the curves is apparently due to a decrease of sensitivity at large optical densities

28

Table 8. Intensities and sensitivities for phosphorus lines in the ultra-violet

λ, Å	Intensity, rel. units*	Sensitivity,† D/M
2 135·47	22	
2 136·18	100	2×10^7
2 149·14	100	
2 152·94	10	$1·25 \times 10^7$
2 154·08	24	
2 533·99	250	
2 535·61	1 000	5×10^5
2 553·25	400	
2 554·90	210	$2·5 \times 10^5$

* Intensity in relative units without taking into account the variations in transmittance of the optical system and photomultiplier sensitivity for various spectrum regions.

† Sensitivity in units of D/M ratio (optical density/g), for 2 700°K, cuvette 2·5 mm in diameter.
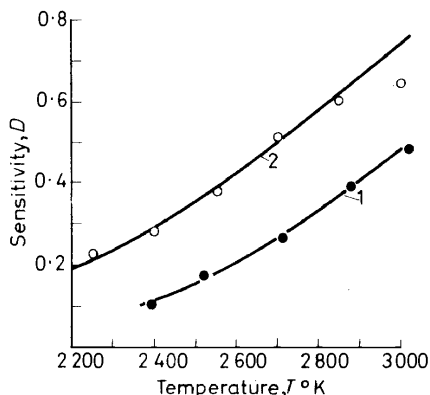
Figure 8. Sensitivity versus temperature. 1—Line P 2 136·18 Å, 2×10^{-8} g; 2—line P 2 061·63 Å, 2×10^{-7} g

(a deviation of the calibration graph from the straight line) and an increase of vapour losses through diffusion at high cuvette temperatures.

Figure 9 presents calibration graphs for both elements obtained at 2 700°K with argon pressure in the chamber at 3 atm in a 2·5 mm diameter cuvette. Records for these elements are shown in *Figure 10*. The detection limit, defined as twice the signal fluctuation magnitude, is 2×10^{-10} g for P and 2×10^{-9} g for I, which is an order of magnitude inferior to the detection limits achieved with the resonance lines. However, with a dosage of 10 µl of solution on the electrode it is possible to detect down to 2×10^{-6} per cent P and 2×10^{-5} per cent I.

Unfortunately, an attempt at sulphur determination by the intercombination line S 1 900 Å (*Table 7*) also lying in the u.v. region of the spectrum was unsuccessful because of an extremely low oscillator strength of this line.

29

The excited state $3d^5D^0$ which is the closest to the ground state of sulphur $3p^3P$ lies at 8·4 eV, and therefore there is no possibility of using non-resonance sulphur lines in atomic absorption spectroscopy in the u.v. region of the spectrum.
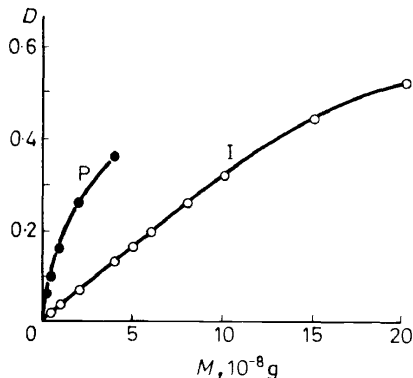
Figure 9. Calibration graphs
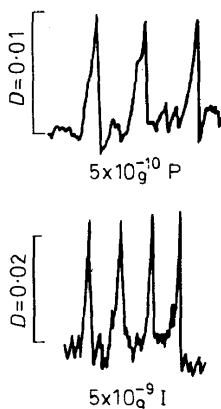
Figure 10. Analytical records

DETERMINATION OF RELATIVE OSCILLATOR STRENGTH FROM ATOMIC ABSORPTION MEASUREMENTS WITH THE FLAME TECHNIQUE

In conclusion I should like to discuss the method of determining relative magnitudes of oscillator strength ensuing from a comparison of sensitivities of various lines in atomic absorption spectroscopy. It may be remembered that the first attempt in this field was made by A. Walsh and co-workers[39] with the purpose of finding oscillator strengths for resonance lines of various elements. However, because of differences in the degree of evaporation and dissociation of the compounds introduced into the flame, as well as different

30

ionization states of atoms of various elements this attempt was not very successful.

A much more effective method should be determination of relative f values for various lines in the spectrum of one element since in this case all the above differences should not be critical. With a pure Doppler line broadening in the flame, the following relationship should hold for all lines in the spectrum of the element in question:

$$f_{ik} \propto \frac{dD}{dC} \frac{1}{\lambda} \frac{1}{g_i \exp(-E_i/kT)} \tag{28}$$

where dD/dC is the sensitivity of atomic absorption measurements at low optical densities (representing a slope of the straight part of the calibration graph); λ is the wavelength of the line to be studied taking into consideration the difference in the Doppler width of the lines lying in different parts of the spectrum; and $g_i \exp(-E_i/kT)$ is a factor accounting for the population of the lower line level at an absorbing layer temperature T.

Assumption of a purely Doppler mechanism of line broadening in high-temperature flames can be considered sufficiently sound for all lines except those of alkali elements, which show a tendency to Lorentz broadening, and the lines of such heavy elements as Hg, Tl and Bi. From our measurements[16], the Voigt parameter $a = (\Delta v_L / \Delta v_D) \sqrt{(\ln 2)}$ usually does not exceed 0·5 to 0·6. For example, for Ag 3281 Å, $a = 0·4$; for Al 3093 Å, $a = 0·3$; and for Fe 2967 Å, $a = 0·5$. One should also take into account the fact that the magnitude of a decreases sharply with line wavelength ($\propto \lambda$) and increasing layer temperature ($\propto T^{-1·2}$).

To check the method, we[40] used it to determine the f values in the spectra of some elements (Cr, Cu, Eu, Fe, Gd, Ge, Si, Sn) for which there exist reliable data obtained by the 'hook' method[29] or by the total absorption technique[30]. The values of dD/dC were taken from published atomic absorption measurements. As an illustration, *Tables 9, 10* and *11* summarize the results of such a comparison for the lines of FeI, GaI and SiI. Good agreement between the data speaks in favour of the method. Altogether, we have calculated by means of this method the f values for 500 lines in the spectra of 40 elements using only sensitivity data taken from the literature. When evaluating the reliability of the f values obtained in this way one should take into account that in most of the work sensitivity measurements were carried out under conditions chosen to be as close as possible to the analytical conditions and far from the optimum from the viewpoint of the determination of f. This remark refers to the operating current of the hollow-cathode lamps (involving self-absorption), monochromator slit width choice, flame geometry, the precision of optical density readings and even publication of the data obtained (when results are rounded off to two or one significant figure). It is evident that taking all the above items into consideration should improve the precision and reliability of determination.

The method can be applied to a study of lines involving transitions to a level located high above the ground state (particularly when using a plasma source which provides higher temperatures than those obtained with the flame technique). Besides neutral atoms, one can investigate also spectra of singly-ionized atoms. The advantages of the method lie in a *wide spectral*

Table 9. Relative f values of the resonance lines for FeI

λ, Å	Low level energy, cm^{-1}	$\dfrac{dC}{dD}$ [33] μg/ml/1%	f_{a-a}	f_h^* [34]	f_h^* [29]	f_{radiat}^* [31]
2166·77	$(3d^64s^2)^5D_4$ (0)	0·50	230	—	—	105
2462·65	(0)	2·42	42	—	—	150
2483·27	(0)	0·10	1000	—	—	540
2501·13	(0)	0·42	240	—	—	170
2522·85	(0)	0·21	470	—	—	470
2719·02	(0)	0·34	270	288	—	240
2936·90	(0)	2·35	36	41·7	42	45
2966·90	(0)	0·82	103	105	—	89
2983·57	(0)	1·26	66	71	112	70
3020·64	(0)	0·37	220	—	—	130
3440·61	(0)	1·65	44	51	—	87
3679·92	(0)	8·9	7·6	7·2	9·1	10
3719·94	(0)	0·67	100	100	82·3	91
3824·44	(0)	8·7	7·6	12·3	—	11
3859·91	(0)	1·12	58	54	54	54

* Reduced to the relative scale for f_{a-a} [34] by using the lines at 3859·91 Å or 3719·94 Å as a reference.

Table 10. Relative f values of the resonance lines for GaI, $T = 2300°$K

λ, Å	Low level energy, cm^{-1}	$\dfrac{dC}{dD}$ [33] μg/ml/1%	f_{a-a}^*	f_h [29]	f_{abs}^* [35]	f_{radiat}^* [31]
2450·08	$(4s^24p)^2P_{1/2}$ (0)	28	0·036	0·038	—	0·14
2500·19	$^2P_{3/2}$ (826)	22	0·037	0·038	—	0·14
2874·24	(0)	2·3	0·37	0·32	0·35	0·28
2943·64	(826)	2·4	0·29	0·29	0·29	0·29
4032·98	(0)	6·2	0·10	0·129	0·11	0·092
4132·05	(826)	3·7	0·13	0·135	0·12	0·10

* Reduced to the absolute scale for f_h by using the line at 2943·64 Å as a reference.

Table 11. Relative f values of the resonance lines for SiI, $T = 2900°$K

λ, Å	Low level energy cm^{-1}	$\dfrac{dC}{dD}$ [36] μg/ml/1%	f_{a-a}	f_h^* [37]	f_{calc}^* [38]	f_{radiat}^* [31]
2207·97	$(3s^23p^2)^3P_0$ (0)	16·3	260	—	—	40
2210·88	$^3P_1$ (77)	7·8	190	—	—	13
2216·67	$^3P_2$ (223)	4·5	200	—	—	14
2506·90	(77)	3·1	420	410	420	370
2514·32	(0)	3·8	1000	1000	1000	1000
2516·11	(223)	1·2	710	710	710	480
2519·21	(77)	5·5	240	260	250	260
2524·11	(77)	4·0	330	340	336	500
2528·51	(223)	3·7	230	250	250	260

* Reduced to the relative scale for f_{a-a} by using the line at 2514·32 Å as a reference.

region covered (down to 1900 Å), possible *application to the majority of elements in the periodic system* including the lowest volatile ones such as W, Zr, Hf, *the absence of any systematic errors* associated with instrument calibration by a spectrum (as is, for example, the case with relative intensity measurements[31]), *simplicity, high speed and widespread use, in which respect this method is vastly superior to other techniques for the measurement of f*.

ACKNOWLEDGEMENTS

REFERENCES

1 S. L. Mandelstam, *Vvedeniye v Spektral'ny Analiz (Introduction to Spectral Analysis),* Gostekhizdat: Moscow (1946).

2 Ya. D. Reichbaum and V. D. Malykh, *Opt. i Spek.* **9**, 425 (1960).

3 A. Angot, Compléments de mathématiques à l'usage des ingénieurs de l'électrotechnique et des télécommunications, *Revue d'optique:* Paris (1956).

4 H. L. Kahn, G. E. Peterson and J. E. Schallis, *At. Absorption Newsletter,* **7**, 35 (1968).

5 R. Woodriff and G. Ramelow, *Spectrochim. Acta,* **23B**, 665 (1968).

6 H. Massmann, *Proceedings of the Second International Symposium, Reinstoffe in Wissenschaft und Technik,* p 297. (1965).

7 Yu. I. Belyaev, L. M. Ivantsov, A. U. Karyakin, Fam Hung Fi and V. V. Shemet, *Zh. Analyt. Khim., Mosk.* **23**, 508 (1968).

8 B. V. L'vov, D. A. Katskov and G. G. Lebedev, *Zh. Prikl. Spektr.* **9**, 558 (1968).

9 B. V. L'vov, *Zh. Prikl. Spektr.* **8**, 517 (1968).

10 H. Massmann, *Méthodes Physiques d'Analyse (GAMS),* **4**, 193 (1968).

11 A. Walsh, *Spectrochim. Acta,* **7**, 108 (1955).

12 B. V. L'vov, *Inzhen-Fiz. Zh.* **2** (No. 2), 44 (1959).

13 B. V. L'vov and G. V. Plyushch, *Zh. Prikl. Spektr.* **10**, 903 (1969).

14 H. Kaiser, *Trace Characterization,* p 154. Edited by W. W. Meinke and B. F. Scribner, *NBS Monograph 100:* Washington (1967).

15 V. P. Borzov, B. V. L'vov and G. V. Plyushch, *Zh. Prikl. Spektr.* **11**, 217 (1969).

16 B. V. L'vov, *Spectrochim. Acta,* **24B**, 53 (1969).

17 B. V. L'vov, *Atomno-Absorptsionny Spektral'ny Analiz (Atomic Absorption Spectroscopy).* Nauka: Moscow (1966).

18 D. A. Katskov and B. V. L'vov, *Zh. Prikl. Spektr.* **10**, 867 (1969).

19 D. A. Katskov, G. G. Lebedev and B. V. L'vov, *Zh. Prikl. Spektr.* **10**, 215 (1969).

20 B. V. L'vov and A. D. Khartsyzov, *Zh. Analyt. Khim., Mosk.* **25**, 1401 (1970).

21 B. V. L'vov and A. D. Khartsyzov, *Zh. Analyt. Khim., Mosk.* **24**, 936 (1969).

22 A. Walsh, *Appl. Optics,* **7**, 1259 (1968).

23 B. V. L'vov, *Opt. i Spek.* **19**, 507 (1965).

24 R. Woodriff, R. W. Stone and A. M. Held, *Appl. Spectrosc.* **22**, 408 (1968).

25 A. Walsh, *Proceedings of the Tenth International Spectroscopy Colloquium,* pp 127–142. Spartan Books: Washington (1963).

26 G. G. Lebedev and B. V. L'vov, *Zav. Labor.* **34**, 1139 (1968).

27 B. V. L'vov and A. D. Khartsyzov, *Zh. Prikl. Spektr.* **11**, 9 (1969).

28 B. V. L'vov and A. D. Khartsyzov, *Zh. Analyt. Khim., Mosk.* **24**, 799 (1969).

29 N. P. Penkin, *J. Quant. Spectr. Radiative Transfer,* **4**, 41 (1964).

30 R. B. King and A. S. King, *Astrophys. J.* **82**, 377 (1935).

31 C. H. Corliss and W. R. Bozman, *Experimental Transition Probabilities for Spectral Lines of Seventy Elements, NBS Monograph 53:* Washington (1962).

32 H. Landolt and R. Börnstein, *Zahlenwerte und Funktionen,* Bd I, Tl 1, Springer: Berlin (1950).

33 W. Slavin, *Atomic Absorption Spectroscopy.* Interscience: New York (1968).

34 A. K. Valters and G. P. Startsev, *Opt. i Spek.* **17**, 483 (1964).

[35] G. M. Lawrence, J. K. Link and R. B. King, *Astrophys. J.* **141**, 293 (1965).

[36] J. S. Cartwright, C. Sebens and D. C. Manning, *At. Absorption Newsletter*, **5**, 91 (1966).

[37] I. Yu. Y. Slavenas, *Opt. i Spek.* **16**, 390 (1964).

[38] P. F. Gruzdev, *Opt. i Spek.* **24**, 860 (1968).

[39] B. J. Russel, J. P. Shelton and A. Walsh, *Spectrochim. Acta.* **8**, 317 (1957).

[40] B. V. L'vov, *Opt. i Spek.* **28**, 18 (1970).

[41] B. V. L'vov and A. D. Khartsyzov, *Zh. Prikl. Spektr.* **11**, 413 (1969).